Molecular Biology of the Cell
Vol. 12, 3439–3450, November 2001

Increased Levels of Keratin 16 Alter Epithelialization Potential of Mouse Skin Keratinocytes In Vivo and Ex Vivo

Matthew J. Wawersik,* Stacy Mazzalupo,* Diem Nguyen, and Pierre A. Coulombe†

Departments of Biological Chemistry and Dermatology, The Johns Hopkins University School of Medicine, Baltimore, Maryland 21205

Submitted April 5, 2001; Revised July 11, 2001; Accepted August 17, 2001
Monitoring Editor: W. James Nelson

The process of wound repair in adult skin is complex, involving dermal contraction and epithelial migration to repair the lesion and restore the skin's barrier properties. At the wound edge, keratinocytes undergo many changes that engender an epithelialization behavior. The type II keratin 6 and type I keratins 16 and 17 are induced well before cell migration begins, but the role of these proteins is not understood. Forced expression of human K16 in skin epithelia of transgenic mice has been shown to cause dose-dependent skin lesions concomitant with alterations in keratin filament organization and in cell adhesion. Here we show, with the use of a quantitative assay, that these transgenic mice show a delay in the closure of full-thickness skin wounds in situ compared with wild-type and low-expressing K16 transgenic mice. We adapted and validated an ex vivo skin explant culture system to better assess epithelialization in a wound-like environment. Transgenic K16 explants exhibit a significant reduction of keratinocyte outgrowth in this setting. This delay is transgene dose-dependent, and is more severe when K16 is expressed in mitotic compared with post-mitotic keratinocytes. Various lines of evidence suggest that the mechanism(s) involved is complex and not strictly cell autonomous. These findings have important implications for the function of K16 in vivo.

INTRODUCTION

Early after injury to the skin, epidermal keratinocytes proximal to the wound edge are mobilized to migrate into the wound site to rebuild the epidermis and restore barrier function (Grinnell, 1992; Clark, 1993; Coulombe, 1997). A process termed activation is believed to endow keratinocytes with the ability to migrate in a coordinated manner (as a stratified sheet) into the wound site. Among the hallmarks of an activated keratinocyte are cell hypertrophy, generation of cytoplasmic processes in the direction of cell migration, altered cell adhesion, and juxtanuclear reorganization of the keratin intermediate filament (IF) network (Coulombe, 1997). Concomitant with these changes, there occurs an induction of the keratin IF proteins keratin 6 (K6), keratin 16 (K16), and keratin 17 (K17) in activated keratinocytes (Mansbridge and Knapp, 1987; Paladini *et al.*, 1996; Machesney *et al.*, 1998; McGowan and Coulombe, 1998b; Takahashi *et al.*, 1998). This induction takes place mostly in the postmitotic compartment of wound edge epidermis, and occurs at the expense of K1 and K10, the major differentiation-specific epidermal keratins. This correlation, along with subsequent analyses, has led to the hypothesis that these keratins play a direct role in preparing keratinocytes for the process of wound epithelialization (Paladini *et al.*, 1996).

Keratins are encoded by a multigene family and are the major structural proteins in vertebrate epithelial cells, where they form an intricate cytoplasmic network of 10-nm IFs. This network is required for the maintenance of cell and tissue integrity in many types of epithelia (Fuchs and Cleveland, 1998). The >40 known keratin genes are highly conserved among mammalian species, and they can be partitioned into types I and II based upon genomic structure and sequence homology (Fuchs and Weber, 1994). The two types of keratin proteins form a heterodimeric coiled-coil as a first step toward polymerization into filaments (Coulombe, 1993). Most keratin genes are regulated in a pairwise, tissue-type, and differentiation-specific manner in vivo, yielding patterns that are conserved throughout mammals. This suggests the existence of a significant relationship between keratin sequence diversity and the structure and function of epithelia. A substantial body of evidence points toward a prominent structural role for type I/type II members of the

* These authors contributed equally to this work.
† Corresponding author. E-mail address: coulombe@jhmi.edu.

IF superfamily (Fuchs and Cleveland, 1998; Magin *et al.*, 1998; Takahashi *et al.*, 1999). However, the large number of keratin genes and their tight differentiation-specific regulation suggest specialized, cell type-specific roles. In support of this notion, transgenic mouse studies show that neither K16 nor the simple epithelial K18 is able to fully complement the skin phenotype exhibited by K14 null mice (Hutton *et al.*, 1998; Paladini and Coulombe, 1999). Moreover, K8 and K18 have been implicated in the response of hepatocytes to various chemical stresses (Ku *et al.*, 1995, 1997; Zatloukal *et al.*, 2000).

We previously reported that directed overexpression of human K16 to either the suprabasal (postmitotic) or basal (progenitor) compartments of epidermis and hair follicle outer root sheath causes dramatic lesions in transgenic mouse skin (Takahashi *et al.*, 1994; Coulombe *et al.*, 1995; Paladini and Coulombe, 1998). Both types of transgenic mice develop alterations in these tissues in a transgene dosage-dependent manner within a week after birth. At the cellular level, these lesions are characterized by cell hypertrophy, changes in cell shape, and alterations in cell adhesion, and in the organization of the keratin IF network. Here, we report that overexpression of human K16 delays the closure of full-thickness skin wounds in vivo. To circumvent limitations inherent to rodent skin and difficulties in quantitating epithelialization from the wound edge, we adapted and validated an explant culture model starting from newborn mouse skin. We show that elevated levels of K16 protein partially impair keratinocyte migration in this model. Our findings have important implications for the functional contribution of K16 during wound repair.

MATERIALS AND METHODS

Transgenic Mouse Lines

All protocols involving mice were approved by the Johns Hopkins University Animal Care and Use Committee (Baltimore, MD). Transgenic mice were generated by pronuclear injection (Hogan *et al.*, 1994) of DNA constructs into B6C3F1 mice. The genome of 5-7-sbK16 and 6-17-sbK16 mouse lines ("sb" implies expression in the suprabasal compartment of epidermis and hair follicle outer root sheath) harbors a human 11-kb DNA fragment comprising full-length K16 coding sequence, ~6 kb of 5′ upstream sequence, and ~1.5 kb of 3′ noncoding sequence (Takahashi *et al.*, 1994). The genome of 10-bK16 mice ("b" implies expression in the basal layer of the same skin epithelia) contains a DNA construct consisting of the human K14 gene promoter (2 kb), a rabbit β-globin intron, the human K16 cDNA, and the 3′ end, including polyA from the human K14 gene (Paladini and Coulombe, 1998). B1-bK16-C14 mice harbor a transgene that uses the same expression cassette to express a chimeric keratin consisting of the head and most of the rod domain of human K16 (368 amino acids) fused with the C-terminal ~105 amino acids of human K14 (Wawersik *et al.*, 1997). KT1-1p mice (Takahashi and Coulombe, 1997) harbor a DNA fragment containing the 5′ upstream region of the human K6a gene, the bacterial *lacZ* sequence (modified to contain a nuclear localization sequence at its 5′ coding end), and the simian virus 40 polyA sequence at its 3′ end (Takahashi and Coulombe, 1996, 1997). Mice were bred and screened as described (Takahashi *et al.*, 1994; Takahashi and Coulombe, 1997; Paladini and Coulombe, 1999).

Primary Antibodies

We used rabbit polyclonal antibodies directed against K6 or K17 (McGowan and Coulombe, 1998a), human K16 (#1275; Takahashi *et al.*, 1994), and mouse K16 (KH anti-K16; our unpublished data), and mouse monoclonal antibodies against K10 (K8.60; Sigma, St. Louis, MO), K14 (LL001; Purkis *et al.*, 1990), and BrdU (BU-33; Sigma).

In Vivo Wound Closure Assay

A quantitative skin wound closure assay was performed as described (Mellin *et al.*, 1995). Briefly, 3-mo-old wild-type and K16 transgenic mice from the 6-17-sbK16 and 5-7-sbK16 lines were coded by a third party and their dorsum depilated with Nair cream (Carter-Wallace, New York, NY). The next day, corresponding to day 0 of the assay, the mice were anesthetized and a full-thickness, 15-mm-diameter, circular skin wound was made in the dorsal trunk. The wound site was kept moist throughout the experiment with the use of Bacitracin ointment (McKesson, San Francisco, CA). Two of us scored the wounds independently on days 1, 3, 5, 7, 9, and 11 afterward by tracing the outline of the wound margin onto a microscope glass slide. The tracings were scanned into a computer with the use of the Photoshop 4.0 software (Adobe Systems, San Jose, CA), and the perimeter length and surface area were quantitated with the use of the MacBAS version 2.5 software (Fuji Medical Systems USA, Stamford, CT). Closure expressed as a percentage of initial area was converted to linear ingrowth from the wound edges as described (Mellin *et al.*, 1995). This transformation allowed expression of closure in each animal as a kinetic rate that was constant as a function of time. The slopes of linear closure curves were determined by regression analysis and analyzed statistically with the use of analysis of variance.

Ex Vivo Skin Explant Outgrowth Assay

Skin from 2-d-old mice was removed and spread flat onto a Petri dish. Explants to be used for immunostaining were placed onto a glass coverslip (Costar, Cambridge, MA), and 0.5 ml of medium was added. Explants to be used for a quantitative outgrowth assay were placed onto untreated 24-well tissue culture plates (Falcon; BD Biosciences, Franklin Lakes, NJ) and 0.2 ml of medium was added. Medium was prepared as described (Rouabhia *et al.*, 1993) with the use of additives as follows (final concentrations): cholera toxin (0.1 nM), epidermal growth factor (10 ng/ml), T3 (2 nM), transferrin (5 μg/ml), insulin (5 μg/ml), hydrocortisone (0.4 μg/ml), penicillin (60 μg/ml), and gentamicin (25 μg/ml). After overnight incubation at 37°C, 5% CO_2, explants were submerged and grown for another 7 d unless specified otherwise. Medium was changed every 2–3 d.

Quantitating Keratinocyte Outgrowth from Skin Explants

To assess keratinocyte outgrowth as a function of time in culture, phase contrast micrographs of explants were recorded on days 1, 2, 3, 5, and 7. Micrographs were scanned into a computer with the use of the Photoshop 4.0 software, and individual scans were overlaid. The boundary of the most distal cells was marked for each day, as was the edge of the explanted tissue. The MacBAS v2.5 software was used to obtain five measurements from the edge of the explant to the leading edge for each time point. Groups of cells were scored as fibroblast or keratinocyte based upon morphological appearance and immunoreactivity at day 8. At each time point, an average distance of outgrowth (in mm) was calculated for each of 14 explants (keratinocyte) or 3 explants (fibroblast). These distances were then plotted versus time in culture, and a best-fit curve was derived (Cricket Graph III software, Islandia, NY). To assess keratinocyte outgrowth after a period of 8 d in culture, explants were fixed and immunostained for K17 as described below. Eight measurements of the distance of outgrowth (i.e., the difference between the leading edge of the outgrowth and the explant edge) were made at equidistant points along the circumference of the explant. Average outgrowth values were calculated from at least five mice from each genotype with approximately four explants per mouse. Statistical

differences between genotypes were estimated with the use of a mixed linear model with random effects. This analysis allows for estimating group means whose components may exhibit internal correlation or clustering. We adjusted for any such covariation in measurements from mice making up a litter and between groups of mice from different litters by entering litter as a random effect, and the genotype as a fixed effect. Differences between genotype groups were then tested by a series of pairwise vector contrasts. All analyses were conducted with the use of Statistical Analysis System (SAS, Cary, NC).

5-Bromo-2′-deoxyuridine (BrdU) Labeling and Pulse Chase Studies

After 3, 6, or 8 d in culture, explants grown on glass coverslips (Costar) were pulse-labeled with 50 μM BrdU (Sigma). Cultures were incubated with BrdU for 2 h, washed three times with phosphate-buffered saline (PBS), and then allowed to grow for 5, 2, or 0 d, respectively (to a fixed total of 8 d in culture). Cells were then fixed and double-immunostained with antibodies to BrdU and K17 as described (see below).

Mitomycin C Treatment and Boyden Chamber Assays

Skin explants were placed into culture then treated with 10 μg/ml mitomycin C (Sigma) at 24, 48, or 72 h. Cultures were treated for 2 h, washed three times with PBS, and supplied with new medium. After a total of 8 d of culture, explant outgrowths were fixed and immunostained with an antibody to K17. Keratinocyte outgrowth was quantitated as described above. To assess the efficacy of mitomycin C treatment, explant cultures were grown on coverslips, and mitomycin C was performed after 24 h in culture. After a total of 8 d, explant outgrowths were labeled with BrdU as described above, fixed, and coimmunostained with antibodies to BrdU and K17. The ability of keratinocytes to migrate through a porous solid phase was assessed in two different settings. First, skin explants were seeded and cultured on the polycarbonate membrane of Transwell tissue culture inserts (Costar). The pore size of this membrane is 8 μm. After 8 d, cells located either on the top or on both sides of the membrane of separate Transwell inserts were removed with a Q-tip (Johnson & Johnson, New Brunswick, NJ). Membranes were fixed and immunostained for K17 to assess keratinocyte migration through the membrane. Second, primary keratinocytes were isolated from 2-d-old mice (Wawersik and Coulombe, 2000) and plated at multiple densities ($10–60 \times 10^4$ cells) in duplicate in the upper chamber of Transwell inserts (Costar). After overnight incubation, unattached cells were removed and fresh culture medium was added. After a total of 77 h in cultures, all Transwell filters were fixed and immunostained for K17 to assess keratinocyte migration through the membrane. Stained preparations were then scanned with the use of the Adobe Photoshop 4.0 software, and densitometry (NIH Image 1.60 software) was performed to quantitate staining intensity. The upper membrane side was then wiped to remove keratinocytes that had not migrated through, the membranes rescanned, and requantitated as described. A migration index was calculated as the ratio of cells having migrated to total cells.

Morphological Studies

Mouse skin tissues were fixed with Bouin's fixative, paraffin-embedded, and 4-μm sections were cut. Antibody staining was performed as described (McGowan and Coulombe, 1998a) with the use of the following antisera: K17 (1/1000), KH anti-K16 (1/400), K16–1275 (1/300), K6gen (1/100), K10 (1/50). A peroxidase-based staining assay was applied as described (Kirkegaard and Perry Laboratories, Gaithersburg, MD). Skin explants grown in culture were washed in PBS and fixed with 3% paraformaldehyde in PBS for 15 min followed by 100% methanol for 4 min. Explants used for the quantitative outgrowth assay were immunostained for K17. To assess the organization of keratin filaments, immunofluorescence microscopy was used (Wawersik and Coulombe, 2000). The skin tissue moiety was carefully removed before staining. Bound primary antibodies (see above) were detected by secondary antibodies conjugated to either rhodamine or fluorescein isothiocyanate (Kirkegaard and Perry Laboratories). For immunostaining of BrdU-labeled keratinocytes, explants were incubated in 1.5 M HCl for 40 min at 37°C before the blocking step. Explants from KT1–1p mice were fixed in 2% paraformaldehyde and 0.1% glutaraldehyde in PBS for 10 min and then incubated with X-gal staining solution (Garlick and Taichman, 1994) at 30°C for 3–8 h.

Electrophoretic Analyses

Cells corresponding to the outgrowth were collected with the use of a cell scraper (Sarstedt, Newton, NC) and boiled in SDS-PAGE sample buffer. Proteins were resolved with the use of an 8% SDS-PAGE gel and either stained with Coomassie blue or transferred to nitrocellulose for Western analysis. Nitrocellulose membranes were blocked with 5% nonfat dried milk in PBS. Subsequent antibody incubations were performed in 0.5% bovine serum albumin (Sigma) and 0.2% Tween 20 (Sigma) in PBS. Western blots were revealed with the use of either peroxidase with enhanced chemiluminescence (Amersham Pharmacia Biotech, Piscataway, NJ) or alkaline phosphatase with 5-bromo-4-chloro-3-indolyl phosphate/nitroblue tetrazolium (Bio-Rad, Hercules, CA).

RESULTS

sbK16 Transgenic Mice Show a Delay in Closure of Full-Thickness Skin Wounds In Vivo

Modest overexpression of the full-length human K16 gene causes follicular keratosis in a dosage-dependent manner in the skin of transgenic mice (Takahashi *et al.*, 1994; Coulombe *et al.*, 1995). Injury to the epidermis of these mice triggers an induction of the transgene in the suprabasal layer of wound edge epidermis, which corresponds to the situation seen for endogenous K16 in human and mouse skin. We used this model to assess the consequences of artificially elevating the levels of K16 in a tissue-specific manner on the wound repair response. Two transgenic lines were subjected to a quantitative wound closure assay in vivo. Mice heterozygous at the transgene insertion site in the 5-7-sbK16 line exhibit a transient skin phenotype that appears at ~7 d after birth, coinciding with the emergence of fur. This phenotype resolves itself within 1 mo. In contrast, line 6-17-sbK16 exhibits subthreshold levels of human K16 expression and never shows a skin phenotype (Takahashi *et al.*, 1994).

We subjected 3-mo-old wild-type (n = 4), 6-17-sbK16 (n = 3), and 5-7-sbK16 (n = 3) mice to the assay described by Mellin *et al.* (1995). Wild-type B6C3F1 mice can consistently close 15-mm-wide full-thickness skin wounds within 10–11 d. Closure proceeds at a steady rate over this time period, and is brought about by two complementary processes (Clark, 1993; Martin, 1997): epithelialization from the wound edges, which involves a combination of enhanced mitotic activity and migration of keratinocytes, and dermis-mediated contraction, which pulls the edges of the wound toward its center. Analysis of serial sections of closed wounds in wild-type mice suggests that the contribution of dermal contraction exceeds 60%.

Relative to wild-type, 5-7-sbK16 transgenic mice show a modest, statistically significant delay (32%) in the rate of

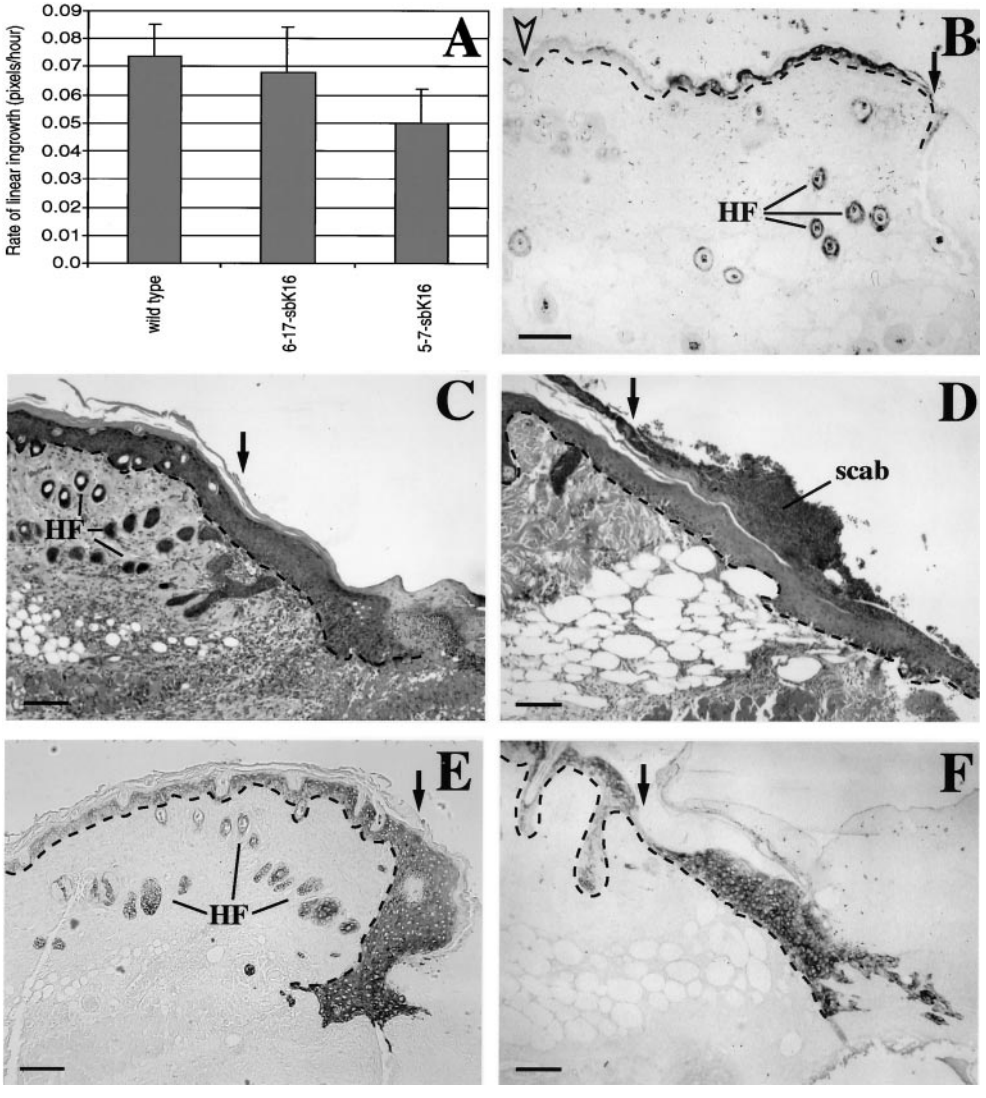

Figure 1. Analysis of full-thickness skin wounds in vivo. (A) In vivo wound closure assay was performed to determine the average rate of linear ingrowth for wild-type (n = 4), 6-17-sbK16 (n = 3), and 5-7-sbK16 (n = 3) mice. Mice from the 5-7-sbK16 line display significantly ($p < 0.04$) slower ingrowth than wild type. The 6-17-sbK16 mice do not vary significantly from wild type. (B–F) Skin wounds were fixed at various time points for histological analysis. C and E show wounds from wild-type mice, whereas B, D, and F show wounds from 5-7-sbK16 mice. Immunostaining with antibodies that preferentially recognize human K16 shows transgene induction 27 h after wounding (B). C and D are hematoxylin and eosin stainings of sections from 5-d-old wounds. E and F are 5-d-old wounds that have been immunostained with antibodies directed against K17. Black arrows denote the wound edge. The open arrowhead shows nonwounded skin, which does not express the transgene (B). HF, hair follicles. Bars, 100 μm.

closure of these full-thickness circular wounds (Figure 1A). The lower expressing 6-17-sbK16 mice are unaffected (Figure 1A). Immunostaining of cross sections through the wound tissue shows that, as expected, the human K16 transgene product is present in the suprabasal layers of epidermis at the edge of skin wounds (Figure 1B). Its expression persists at the wound edge and in the migrating epithelium at later times. Similar results are seen in 6-17-sbK16 mice. Hematoxylin and eosin staining of paraffin-embedded sections made through the middle of the wound site at 7 d after injury shows that, compared with wild-type controls (Figure 1C), the wound epithelium of 5-7-sbK16 trangenic mice does not exhibit any obvious and consistent changes (Figure 1, D and F). No evidence of cell lysis can be detected, consistent with our previous characterization of spontaneous skin lesions in these mice (Takahashi et al., 1994; Coulombe *et al.*, 1995). Likewise, no difference can be detected in similar wound sections prepared from wild-type, 6-17-sbK16, and 5-7-sbK16 mice and immunostained for K17 (Figure 1, E and F), endogenous K16, K6, or K10 antigens.

Validation of a Skin Explant Culture Assay to Study Epithelialization

Owing in part to the dominant contribution of the dermis-mediated contraction, and in part to the fragility of the wound epithelium when preparing histological sections, it is difficult to assess, in a quantitative and reliable manner, the process of wound epithelialization in adult mouse skin in situ. To circumvent these limitations and enable further characterization of the wound repair phenotype shown by 5-7-sbK16 mice, we adapted and validated an ex vivo skin explant culture system in which epithelialization is seen to occur in a manner remarkably similar to a wound site in adult skin.

When full-thickness skin biopsies are seeded into primary culture and allowed to attach to the substratum, keratinocytes soon emerge from its edges and "colonize" the proximal environment (Lampe *et al.*, 1998). We tested whether this epithelialization process was related to that seen after skin injury in vivo. Within 24 h of placing a 4-mm full-

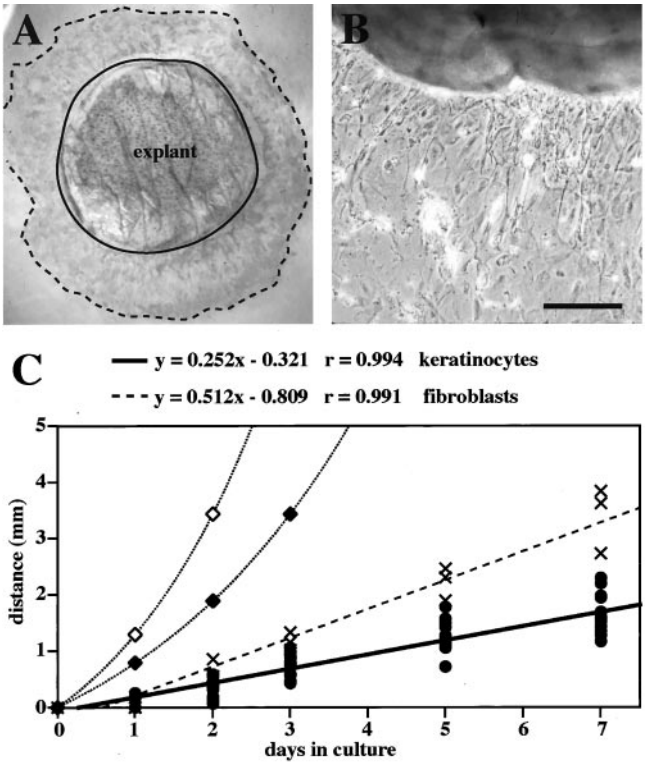

Figure 2. Analysis of explants from newborn mice. (A) A 4-mm full-thickness punch biopsy was isolated, grown in medium for 7 d, and immunostained with antibodies directed against K17 to confirm the cells are keratinocytes. The solid line denotes the explant edge. The dotted line denotes the cells that are most distal to the explant. (B) Phase contrast microscopy of an unstained explant. Cells that have migrated onto the culture dish have an epithelioid appearance. Bar, 200 μm. (C) Distance between the explant edge and the most distal cells of the outgrowth was measured over time. The heavy solid line is a linear curve fit to the keratinocyte measurements (●). The dashed line is a linear curve fit to measurements of fibroblast outgrowth (×). A 24-h (◇) or 36-h (◆) cell cycle time was used to calculate the theoretical curve for distance due to cell proliferation, distance = $(A_{total}/\pi)^{1/2} \cdot (e^{t/2\tau})$.

thickness punch biopsy from 2-d-old mouse skin into medium, cells begin to grow "away" from the edge of the explant tissue. This epithelial outgrowth is sustained over a period of at least 8 d (Figure 2, A and B) and depends upon the presence of both dermis and epidermis in the explant. Mazzalupo, unpublished data).

The two major factors that could contribute to the movement of keratinocytes away from the edge of the explant tissue are cell proliferation and migration. Cell proliferation would push the cells as they continue dividing and thus cell expansion would occur exponentially based upon the length of the cell cycle. Migration would be expected to lead to a more linear rate of outgrowth. We measured the rate of keratinocyte outgrowth over a 7-d period in wild-type skin explants. This was also done for fibroblasts, given that we occasionally obtained explants for which they represented the primary cell type growing out of them. A curve fit to the keratinocyte data gave a linear rate of 0.23 mm/d (Figure 2C). Fibroblast outgrowth could also be fitted to a linear curve, but exhibited a steeper slope. These curves were compared with the theoretical exponential curves expected for expansion fueled through mitosis with population doubling times of 24 h (Missero *et al.*, 1996) or 36 h. In both cases, the observed rates for keratinocytes failed to approach these rates.

To further assess the mechanism(s) responsible for outgrowth from explants, we monitored keratinocyte movements by pulse-chase labeling, in a modified Boyden chamber assay, and after mitomycin C treatment. Proliferating keratinocytes from wild-type explant cultures were pulse-labeled with BrdU after 3, 6, or 8 d in culture then allowed to grow another 5, 2, or 0 d, respectively. The majority of BrdU-labeled keratinocytes in explant cultures are located proximal to the explant (Figure 3, A and D), allowing us to track the movement of labeled cells with respect to the explant edge during the chase period. After BrdU incorporation at day 6 and a 2-d chase period, the majority of BrdU-positive keratinocytes were found primarily in the middle of the explant outgrowth (Figure 3, B and E). Likewise, incorporation at day 3 followed by a 5-d chase showed that most BrdU-labeled keratinocytes were localized to the most distal edge of the explant outgrowth (Figure 3, C and F). Similar results were obtained by pulse-labeling with the endoplasmic reticulum-specific dye DiI. These data suggest that a significant fraction of the incorporated BrdU is not getting diluted by successive mitoses during the chase and that keratinocytes are migrating away from the explant itself.

To simulate a Boyden chamber assay, explant cultures were grown on a polycarbonate support membrane with 8-μm pores. This did not overtly affect keratinocyte outgrowth (Figure 3G). Removal of cells from one or both sides of the porous membrane showed that keratinocyte outgrowth occurred on both sides (Figure 3, compare H and I). This implies that keratinocytes had actively migrated through the 8-μm pores over the course of the assay. Furthermore, phase contrast microscopy revealed that some keratinocytes (as confirmed by K17 immunostaining) and fibroblasts were growing directly on the plastic tissue culture dish (Figure 3J).

Finally, we allowed keratinocyte outgrowth to continue after permanently blocking cell proliferation with mitomycin C (Figure 3K). This treatment was performed for 2 h at 24, 48, and 72 h after the explants were placed in culture. After incubation, cultures were washed and maintained for a total of 8 d. We determined that >97% of cell proliferation was blocked by mitomycin C (data not shown). Compared with untreated controls, the amount of keratinocyte outgrowth (as measured by distance from the explant edge) was reduced by ~52% when mitomycin C treatment was done at 24 h. Outgrowth was reduced by ~43 and ~17% when treatment was performed at 48 or 72 h, respectively (Figure 3K). This set of experiments indicates that proliferation and migration both contribute to keratinocyte outgrowth from wild-type explants.

We next analyzed the distribution of keratin antigens in explant cultures to assess whether it mimics that seen in wound edge keratinocytes in vivo. We immunostained for the basal epidermis-specific K14, the differentiation-specific K10, as well as K6, K16, and K17. We found that K6, K14,

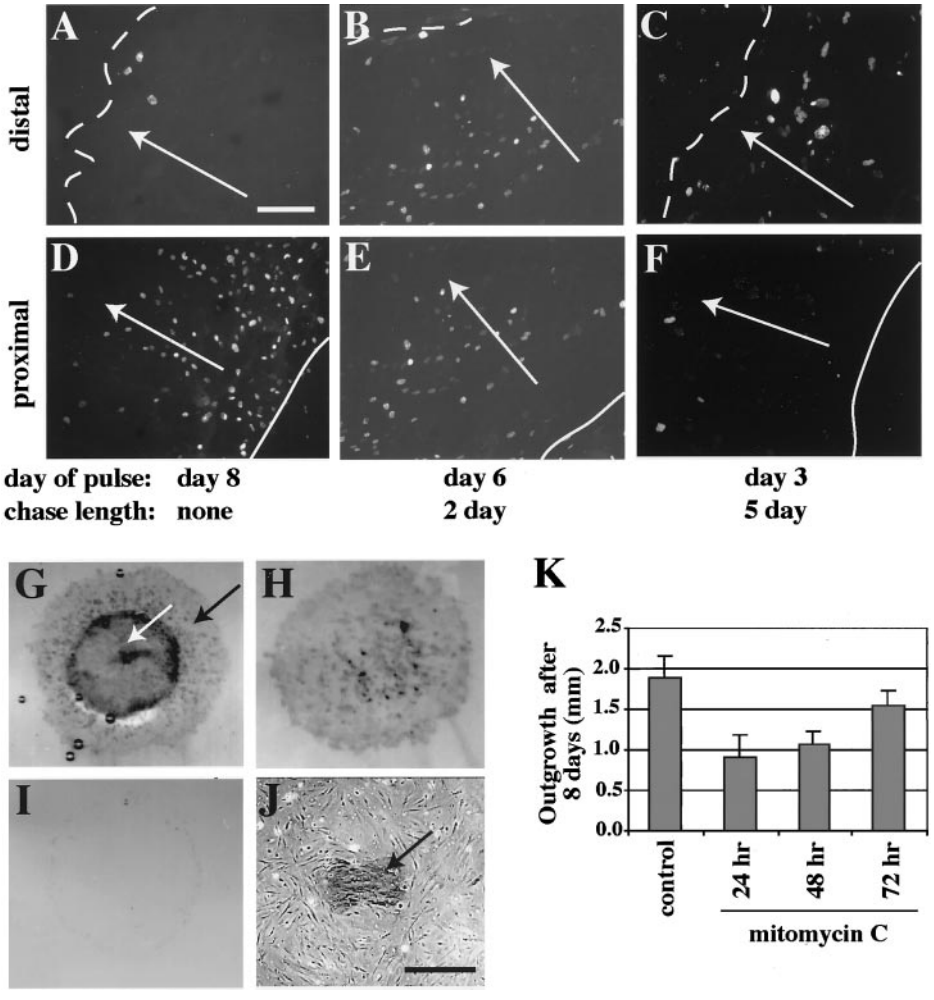

Figure 3. BrdU pulse-chase labeling of skin explants. (A–F) Keratinocyte outgrowth from wild-type explants was pulse-labeled with BrdU after 3, 6, or 8 d of culture, fixed after a 5-, 2-, or 0-d chase period, respectively, then immunostained to assess movement of BrdU-positive cells over time. (A and D) BrdU labeling after 8 d, with no chase, shows that most BrdU-positive keratinocytes localize proximal (solid line) rather than distal (dotted line) to the explant. Labeling after 6 d of culture followed by a 2-d chase (B and E), or after 3 d with a 5-d chase (C and F), reveals that the majority of BrdU-positive keratinocytes have moved away from the proximal explant edge (E and F) and closer to the distal edge (B and C). White arrows indicate the direction of outgrowth movement. Bar, 170 μm. (G–J) Modified Boyden chamber assay. Wild-type explants were cultured on a porous membrane for 8 d, fixed, and immunostained for K17 to assess migration of keratinocytes through the membrane. After immunostaining, keratinocytes were removed from the bottom, top, or both sides of the membrane. Outgrowth of keratinocytes (black arrow) out of the explant (white arrow) appeared normal on top of the membrane (G). Keratinocytes were also observed to have moved through membrane pores and localized on the bottom side of the membrane (H) as well as on the culture dish below the membrane (black arrow) alongside fibroblasts (J). Wiping both sides of the membrane shows cell removal to be efficient (I). Bar, 300 μm. (K) Mitomycin C treatment. Keratinocyte outgrowth after 8 d in culture was quantitated for wild-type explants previously treated with mitomycin C to permanently block cell proliferation. Treatment was performed for 2 h at either 24, 48, or 72 h after explants were placed into culture, and resulted in an ~48, ~43, and ~17% reduction in keratinocyte outgrowth, respectively.

K16, and K17 are all present in the keratinocyte outgrowth (Figure 4, A–D). The staining patterns for K14, K17, and K6 were fairly homogeneous throughout the outgrowth. K16 antigens were detected throughout the explant outgrowth as well, although with a greater cell-to-cell variability in staining intensity (Figure 4B). In contrast to these antigens, K10 exhibited only a dim, nonfilamentous signal (Figure 4E). The reduced content of K10 in explant outgrowth compared with primary cultures of newborn mouse keratinocytes, where a subset undergoes spontaneous differentiation, was confirmed by Western analysis of total protein extracts (Figure 4F). These experiments show that the distribution of keratin antigens in the explant outgrowth is very similar to that seen in skin wound sites in situ (Paladini *et al*., 1996; McGowan and Coulombe, 1998a; Takahashi *et al*., 1998; Wojcik *et al*., 2000).

We also exploited a transgenic mouse line, designated KT1–1p, whose genome harbors a DNA construct consisting of the 5′ upstream sequence of the human K6a gene fused to the bacterial *lacZ* sequence modified with a nuclear localization signal (Takahashi and Coulombe, 1996; Takahashi and Coulombe, 1997). This upstream region contains elements that confer wound inducibility, as can be seen at the edge of skin wounds in vivo (Figure 4G). Similarly, as early as 8 h after seeding punch biopsies obtained from KT1–1p newborn skin in explant culture, we observe a strong induction of β-galactosidase activity at the tissue edge (Figure 4H). At later times in culture, reporter expression is maintained at the explant edge and is prevalent throughout the keratinocyte outgrowth (Figure 4I). Based on these findings, the regulation of K6 gene expression may involve similar transcriptional mechanism(s) in the explant culture setting and in skin wounds in vivo.

Together, these studies establish that keratinocyte outgrowth from skin explants ex vivo exhibits several features in common with wound edge tissue in situ. These include migration in the form of a stratified sheet (electron microscopy data), a partial dependence on mitosis, an up-regulation of K6, K16, and K17 at the expense of K1 and K10, and possibly shared mechanisms of K6 gene induction. This

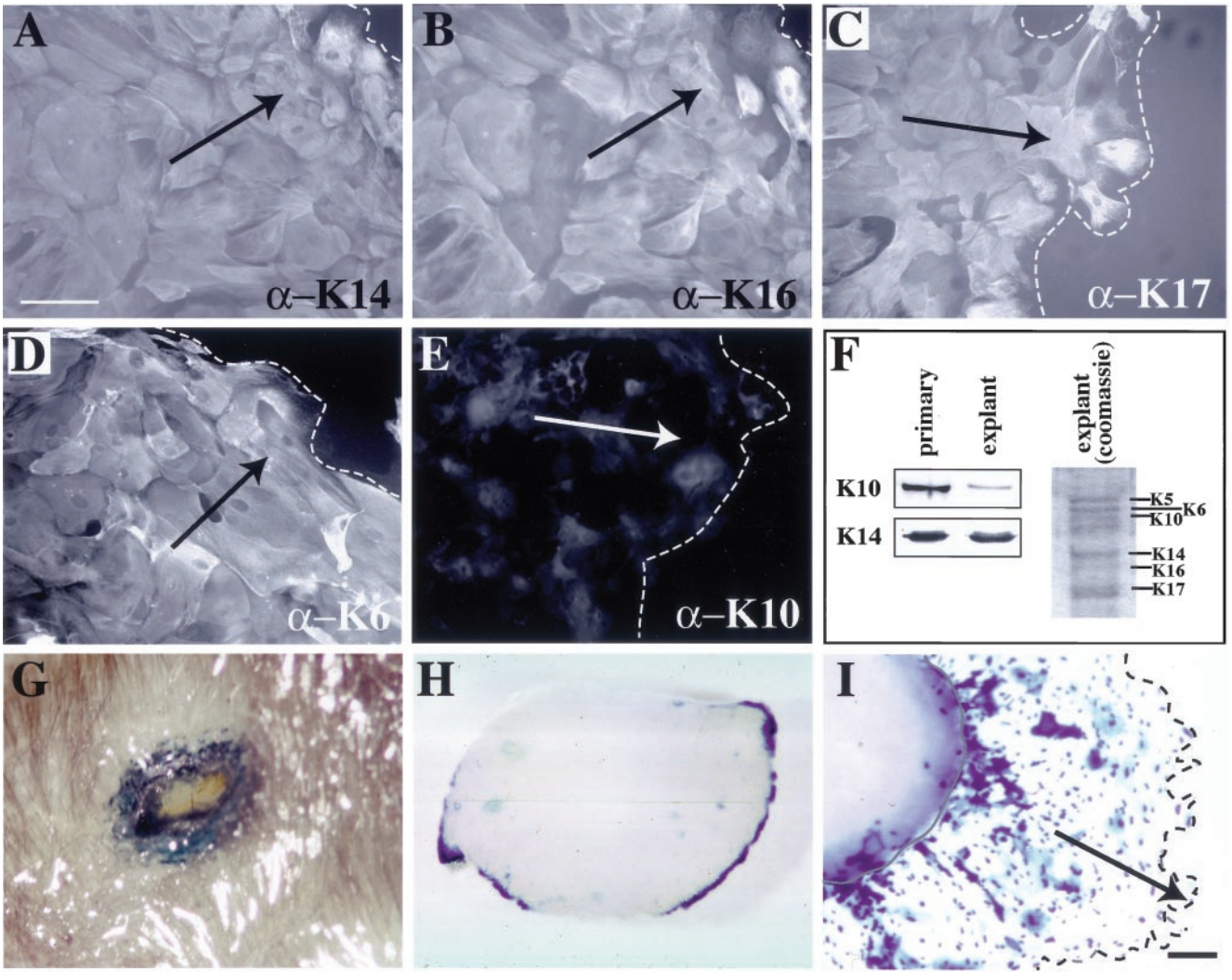

Figure 4. Keratin expression in skin explants. (A–F) Immunofluorescence antibody staining of explant outgrowth. A filamentous pattern is seen for K14 (A), K16 (B), K17 (C), and K6 (D). K6, K17, and K14 staining appears homogeneous throughout the outgrowth, whereas K16 shows a heterogeneous pattern. Only background staining is seen for K10 (E). Bar, 85 μm. Dashed line indicates the distal edge of the outgrowth. Arrows indicate the direction of cell migration. (F) SDS-PAGE and Western analysis show that levels of K10 are decreased relative to K14 in the explant keratinocytes compared with keratinocytes grown in primary culture. (G) X-gal staining of a skin puncture wound in an adult KT1–1p mouse whose genome harbors a wound-inducible promoter fused to *lacZ*. This piece of skin was fixed and stained 24 h after wounding. The blue color indicates β-galactosidase activity. (H and I) Explants were removed from KT1-1p mouse pups, placed into culture, and incubated with X-gal until blue color developed. At 8 h (H), there is already strong induction of the transgene at the edge of the tissue. By 6 d (I) in culture, the cells that have grown out of the explant, and the explant wound edge itself, are positive for the transgene. Bar, 200 μm.

assay offers the advantages of being quantitative and focusing mainly on epithelialization. Because this assay can be conducted with the use of newborn (shown here) or adult mouse skin, it also offers a temporal flexibility that may help circumvent difficulties arising from severe or lethal phenotypes associated with gene manipulations in mice.

Impact of Elevated K16 Levels on Keratinocyte Migration in Ex Vivo Skin Explant Model

We used the explant culture assay to test the epithelialization potential of homozygous 5-7-sbK16 transgenic skin compared with wild-type mouse skin. Quantitation of average outgrowth shows a 30% reduction in sbK16 explants compared with wild-type; a statistically significant difference (Figure 5). This suggests that the source of wound closure delay measured in 5-7-sbK16 mice in vivo (Figure 1) lies in the epithelial and not the connective tissue component of the response.

We next tested for epithelialization in a transgenic mouse model in which the human K16 coding sequence is placed under the control of the K14 promoter (Paladini and Coulombe, 1998). Like sbK16 mice, 10-bK16 mice show epithelial-

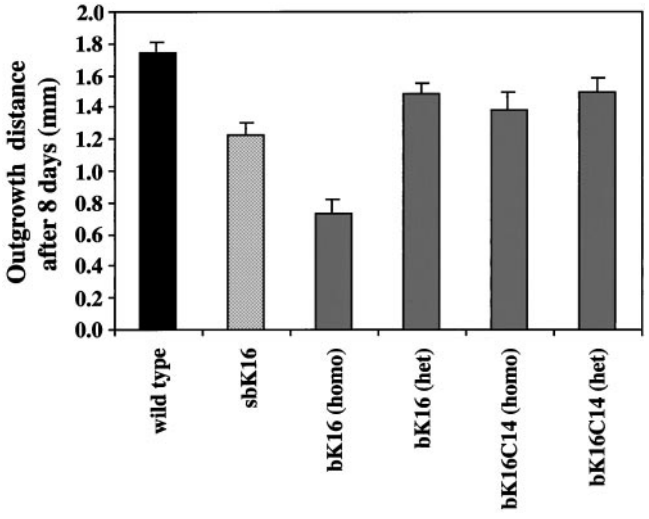

Figure 5. Effect of keratin transgene expression on keratinocyte migration in the skin explant setting. Outgrowth of keratinocytes from wild-type or transgenic explants was quantitated after 8 d in culture. Homozygous 5-7-sbK16 explants show a 30% reduction compared with wild-type explants, whereas homozygous 10-bK16 explants show a 57% reduction. In comparison, explants isolated from heterozygous 10-bK16 and homozygous or heterozygous B1-bK16-C14 mice reveal only a 15, 20, and 15% reduction in outgrowth relative to wild-type, respectively.

specific regulation of human K16, with the exception that expression occurs in the progenitor basal layer as opposed to the suprabasal compartment. These bK16 mice also develop a striking skin phenotype in a dose-dependent manner starting a few days after birth (Paladini and Coulombe, 1998). This is in contrast to mice expressing a chimeric K16-K14 cDNA at comparable levels (Paladini and Coulombe, 1998). We found that explants from 10-bK16 mice show a dramatic, transgene dose-dependent reduction in the amount of keratinocyte outgrowth compared with wild-type (Wawersik and Coulombe, 2000; Figure 5). The reduction is more severe in explants from homozygous transgenic mice, which show twice as much expression as heterozygous mice. B1-bK16C14 transgenic explants, whether homozygous or heterozygous, exhibit modest albeit statistically significant reductions in the amount of keratinocyte outgrowth compared with wild-type skin (Figure 5). The use of a mixed linear model with random effects, a statistical analysis suitable for this experimental design (see MATERIALS AND METHODS), reveals that we can rank order the types of explants into distinct groups as follows: 1) wild-type; 2) heterozygous 10-bK16 and B1-bK16C14, and homozygous B1-bK16C14; 3) 5-7-sbK16; and 4) homozygous 10-bK16 (Figure 5). The reduction in outgrowth observed in homozygous 10-bK16 explants appears to result from a partial impairment of both proliferation and migration, as suggested by experiments involving mitomycin C treatment. In both wild-type and transgenic explants, epithelial outgrowth was inhibited to a similar extent (~50%) when explants were treated with this agent at 24 h after seeding.

We next investigated whether differences in human K16 protein levels and/or distribution could account for the different degrees of inhibition observed in 5-7-sbK16 (30%) and 10-bK16 (57%) explants relative to wild-type. For this purpose, we used the K16–1275 antibody, which recognizes human K16 with higher affinity than mouse K16 (Bernot, personal communication). When subjecting total protein extracts to Western analysis, the amounts of human K16 antigen are comparable in 5-7-sbK16 and homozygous 10-bK16 transgenic explants relative to endogenous K14 (Figure 6A). We then compared the distribution of human K16 and morphology of keratin IF networks with the use of immunofluorescence microscopy. With the use of limiting dilutions of K16-1275, we were able to assess the localization of human K16 with limited interference from mouse K16. Two major differences were observed. First, the 5-7-sbK16 explant outgrowth shows considerably more cell-to-cell variability in staining intensity, especially at locations distal to the explant tissue (Figure 6, compare B and C). Second, differences were seen in the location of keratinocytes showing altered keratin organization within the outgrowth. 5-7-sbK16 skin explants displayed keratin fragmentation in cells located preferentially near the explant edge (Figure 6, compare C and D). In contrast, the subset of keratinocytes showing altered keratin organization in homozygous 10-bK16 skin explants was located more distally (Figure 6C). Alterations in keratin organization were not seen in the other type of transgenics nor in wild-type explants.

Finally, we compared the ability of individual skin keratinocytes in primary culture to migrate through a porous membrane. Wild-type and homozygous 10-bK16 keratinocytes were isolated from 2-d-old pups and plated at a range of cell densities in an attempt to adequately compensate for the modest plating defect exhibited by the latter cells (Wawersik and Coulombe, 2000). After 3 d in culture, we found that in both instances the same fraction of wild-type (52 $\pm$ 16%) and transgenic (53 $\pm$ 7%) keratinocytes had crossed the 8-μm pore filter. These findings imply that the reduced outgrowth exhibited by K16 transgenic explants is not due to a cell autonomous impairment of keratinocyte migration.

DISCUSSION

Cultured Skin Explants as a Model to Study Epithelialization of Wound Sites

The source of keratinocytes responsible for wound resurfacing is the activated epithelium at the wound edge (Clark, 1993; Coulombe, 1997; Martin, 1997). The cellular events driving wound epithelialization are active cell migration into the wound site and enhanced mitotic activity behind the migrating front. The epithelium migrates as a stratified sheet at the interface between the scab and the underlying fibrin- and fibronectin-rich extracellular matrix that has formed soon after injury (Krawczyk, 1971). Examination of histological sections through skin wound sites shows that the epithelial sheet is loosely adherent to the extracellular matrix (our unpublished data). Weaker adhesion is consistent with the newly acquired motile properties of the cells involved in wound epithelialization (Jacinto *et al.*, 2001). Along with the spatial complexity of the wound site, these features make it very difficult to reliably quantitate wound epithelialization from the study of histological sections.

Another complication arises when studying wound repair in mouse and rat skin. Rodent skin is significantly more efficient than human skin in its ability to close skin wounds

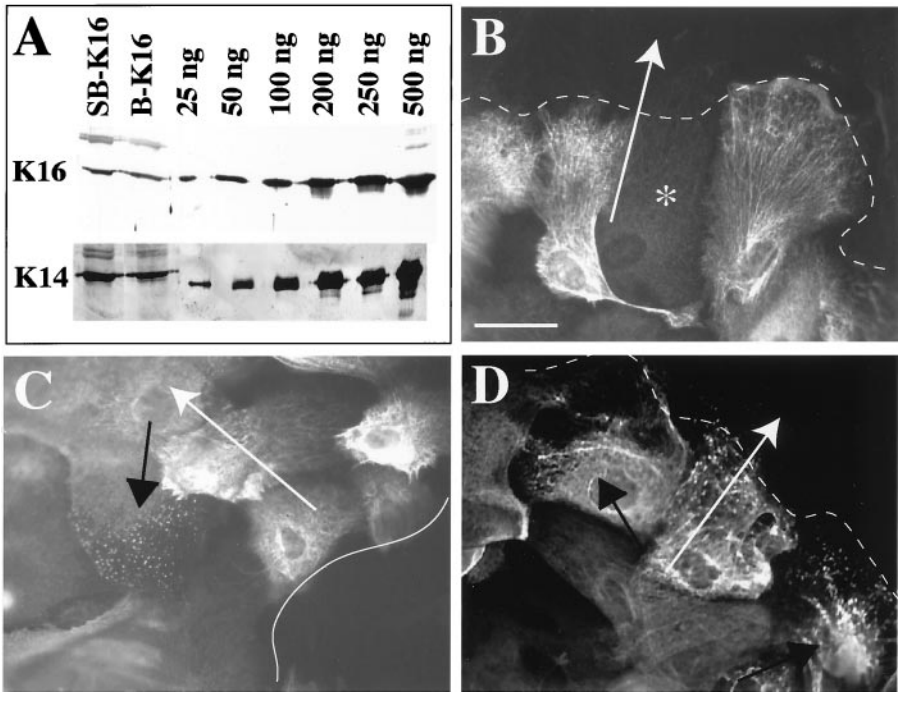

Figure 6. Characterization of K16 expression in transgenic explants. (A) Cell extracts isolated from homozygous 5-7-sbK16 and 10-bK16 explant outgrowth were isolated and subjected to Western analysis. Blots probed with antibodies directed toward K14 and K16 reveal total levels of the hK16 transgene to be similar between keratinocytes from these two types of transgenic explants. (B–D) The distribution and filament reorganizing properties of the hK16 transgene product in homozygous 5-7-sbK16 and 10-bK16 explants were assessed via immunofluorescence. (B) Heterogeneity of hK16 staining at the distal edge of 5-7-sbK16 explants. The asterisk identifies a nonreactive keratinocyte. (C) hK16 staining is less heterogeneous at the proximal edge in these explants, but a subset of keratinocytes shows a punctate staining pattern, indicating alterations in keratin assembly or organization (black arrow). (D) Immunostaining for hK16 in keratinocytes from 10-bK16 explants reveals filament reorganization (black arrows) almost exclusively in keratinocytes distal to the explant as well as a more homogeneous transgene expression pattern throughout the outgrowth. Solid lines indicate the proximal explant edge, dotted lines the distal edge, and white arrows indicate the direction of keratinocyte migration. Bar, 42.5 μm.

largely because of a much greater efficiency of the dermis-mediated wound contraction (Cohen and Mast, 1990; Clark, 1993; Martin, 1997). Contraction pulls the edges of the wound closer together, reducing the distance that migrating epithelial cells have to cover to restore epithelial continuity. This contribution is so dominant that fairly large experimental wounds must be made to enable an assessment of the behavior of epithelial cells after injury to adult mouse skin (Mellin *et al.*, 1995).

The skin explant culture system described here offers great promise as an alternative setting to study the potential of keratinocytes for wound epithelialization. Unlike "scrape wounding" of confluent monolayers of skin keratinocytes in primary culture (Mazzalupo, unpublished data), this explant model involves epithelialization as a stratified sheet, a dependence on both cell migration and mitosis, and appropriate changes in keratin gene expression. Time-lapse recordings of the outgrowth process indicate that keratinocytes are moving as a multicellular sheet (Mazzalupo, unpublished data). Studies involving the sbK16 transgenic mouse model suggest that the behavior of skin keratinocytes in the explant setting is similar to that seen in vivo. This skin explant assay offers several advantages over in vivo studies, including ease of quantitation, the ability to circumvent skin phenotypes that could complicate the interpretation of the findings, less suffering to the animals, and a method to study events in real time with the use of transgenic mice with green fluorescent protein-tagged molecules. The main disadvantages of the ex vivo explant assay are that the provisional tissue matrix and much of the blood-derived inflammatory effectors are absent, and the migrating epithelial sheet exhibits fewer layers ex vivo than in vivo.

Implications for Role of K16 during Wound Repair

The physiological relevance of our finding that artificially elevated levels of human K16 protein delays the epithelialization of skin wounds is unclear. This effect is likely due to the protein itself because an inhibition is observed, albeit to a varying degree, when transgenic K16 expression is regulated by two distinct promoters. This inhibition does not require much transgene overexpression, because human K16 levels less than endogenous K14 suffice to produce a reduction in outgrowth. The effect is not a simple function of elevating the levels of a type I keratin in keratinocytes. Although the bK16-C14 transgenic explants show slightly reduced epithelialization, a stronger effect on epithelialization requires that the C-terminal region of K16 be included in the transgenic protein. Finally, we and others showed that the properties of mouse and human K16 are conserved (Porter *et al.*, 1998; our unpublished data). Given all this, our findings are likely to reflect the true consequences of elevating K16 protein levels in migrating keratinocytes.

Rapid induction of K6, K16, and K17 after acute injury is a response exhibited by many complex epithelia and conserved from amphibians to mammals (McGowan and Coulombe, 1998b). We previously postulated that the induction and subsequent accumulation of K16 protein assist in the process of keratinocyte activation (Paladini *et al.*, 1996) and thus would be expected to impact positively on epithelialization. Here, we observed that elevated levels of K16 protein have the opposite effect. Two arguments can be offered to explain this outcome. First, wound-activated keratinocytes may be very sensitive to the stoichiometry between K6, K16, K17, and the other keratins they contain. Disruption of this delicate balance, such as was done in this study, may be

responsible for converting a positive effect on migration into a negative effect. In support of this, disruption of the molar ratio between the light, medium, and heavy subunits of neurofilament proteins has serious consequences for their assembly and function in neurons (Julien, 1999). Alternatively, induction of K6, K16, and K17 after injury may represent a compromise between a need to maintain mechanical resilience and a requirement for cytoskeletal plasticity during cell migration. Accordingly, the K6/K16/K17 system would provide a level of mechanical scaffolding that is intermediate between K5/K14 and K1/K10, while conferring more plasticity to the keratinocytes than K1/K10. This compromise would result in the acquisition of suitable mechanical stability (Ma *et al.*, 2001) at the cost of a slight delay in epithelialization. Resolving which of these two possibilities, or yet others, is valid will require that additional studies be performed.

In addition to understanding why K16 overexpression delays epithelialization, we would also like to know how K16 functions to cause this delay. One obvious possibility is the dosage-dependent reorganization of keratin filaments promoted by K16 (Wawersik and Coulombe, 2000; this study). We found that the promoter driving human K16 expression had an impact on the preferential localization of keratinocytes showing disrupted IF networks within the epithelial outgrowth. Actively migrating tissue at the leading edge of the epithelial tongue could be more sensitive to keratin IF disruption than the tissue behind it. Based upon experiments involving mitomycin C, elevated K16 levels partially inhibit both mitotic activity and cell migration within skin explants. This said, the outcome of the Transwell migration assay involving individual keratinocytes suggests that impaired epithelialization potential of K16 transgenic explants is not owing to a cell autonomous defect in keratinocyte migration. These observations are consistent with a role for keratin filaments in integrating keratinocytes into a supracellular network; in this particular instance, increased levels of K16 may disrupt cell-cell coordination or affect the ability of keratinocytes to appropriately respond to explant-derived signals. Of note, we previously showed that the skin of 10-bK16 transgenic mice exhibit an increase in tyrosine phosphorylation of EGF receptor before the appearance of a phenotype (Paladini and Coulombe, 1998). This receptor is activated in wound edge keratinocytes shortly after injury to the skin (Stoscheck *et al.*, 1992), and this pathway has been shown to play a role during wound epithelialization (Chen *et al.*, 1993; Fang *et al.*, 1999; Pilcher *et al.*, 1999). Further studies are necessary to elucidate the mechanism(s) involved.

Intermediate Filaments and Response to Tissue Injury

Manipulation of the levels of specific keratins has been shown to alter the response to tissue injury or the ability of epithelial cells to migrate in a tissue setting. Inactivation of the K6α gene has been reported to delay the epithelialization of partial-thickness skin wounds from hair follicles. Epithelialization from the wound margins, the only possible source of cells for the resurfacing of full-thickness skin wounds, is not affected in these mice (Wojcik *et al.*, 2000). How these findings relate to our own involving K16 is unclear at present. The impact of K8 and K18 expression on cell migration was examined in cell culture studies. Elevated levels of K8-K18 correlate with increased migration potential in melanoma cell lines and in transfected mouse L cells (Chu *et al.*, 1993, 1996). In contrast, wound closure is unaffected by a null mutation in K8 when the embryonic ectoderm is experimentally injured (Brock *et al.*, 1996). In this case, however, the notion that K8 is a dominant type II keratin in the embryonic day 11.5–12.5 skin tissue can be challenged (Byrne *et al.*, 1994; McGowan and Coulombe, 1998a). At another level, adult transgenic mice expressing a dominant-negative K18 mutant are more likely to die after partial hepatectomy or other forms of acute challenges (Ku *et al.*, 1996, 1998). The same observation has been made in mice carrying a null K8 allele (Zatloukal *et al.*, 2000). It is clear, therefore, that keratins can influence tissue repair or cell migration in a number of specific settings in vivo and ex vivo.

Several studies have examined the role of nonkeratin IF proteins in response to tissue injury. Dermis-mediated wound contraction is impaired in the absence of vimentin, the major IF protein in connective tissue fibroblasts, leading to a delay in skin wound closure (Eckes *et al.*, 1998). Ex vivo, vimentin null fibroblasts migrate less efficiently and cannot mediate the contraction of collagen gels to the same extent as wild-type cells, suggesting that they are mechanically challenged (Eckes *et al.*, 1998). Acute injury to the CNS is followed by a reactive gliosis, a phenomenon where nearby astrocytes become activated and migrate into the wound site. Activated astrocytes induce the expression of vimentin and nestin while maintaining that of glial fibrillary acidic protein, which they express under normal conditions (Galou *et al.*, 1996; Pekny *et al.*, 1999). Finally, Pekny *et al.* (1999) describe an abnormal repair response of glial fibrillary acidic protein/vimentin double null mice after injury to the CNS and/or spinal cord. Along with ours, these studies establish the notion that IF gene expression typically changes after tissue injury and that newly made IF proteins contribute to shape the response of the cellular effectors involved. Continued studies of the properties and functions of IF proteins in the context of tissue repair should continue to provide insights into the function of the members of this multigene family.

ACKNOWLEDGMENTS

We thank George Melikan for statistical expertise, Angela LeBrun for histology, Kelsie Bernot (our laboratory) for producing the rabbit anti-K16 antiserum, and Dr. Irene Leigh (London, United Kingdom) for providing other useful antibodies. Also, thanks to David Elliott for assistance with preparation of sections for electron microscopy. These studies were supported by grants AR44232 and AR42047 (to P.A.C.) from the National Institute of Arthritis, Musculoskeletal and Skin Diseases/National Institutes of Health.

REFERENCES

Bereiter-Hahn, J. (1986). Epidermal cell migration and wound repair. In: Biology of the Integument, Vol. 2, Vertebrates, ed. J. Bereiter-Hahn, A.G. Matoltsy, and K.S. Richards, Berlin: Springer-Verlag, 443–471.

Brock, J., McCluskey, J., Baribault, H., and Martin, P. (1996). Perfect wound healing in the keratin 8 deficient mouse embryo. Cell Motil. Cytoskeleton *35*, 358–366.

Byrne, C., Tainsky, M., and Fuchs, E. (1994). Programming gene expression in developing epidermis. Development *120*, 2369–2383.

Chen, J.D., Kim, J.P., Zhang, K., Sarret, Y., Wynn, K.C., Kramer, R.H., and Woodley, D.T. (1993). Epidermal growth factor (EGF) promotes keratinocyte locomotion on collagen by increasing the α2 integrin subunit. Exp. Cell Res. *209*, 216–223.

Chu, Y.W., Runyan, R.B., Oshima, R.G., and Hendrix, M.J. (1993). Expression of complete keratin filaments in mouse L cells augments cell migration and invasion. Proc. Natl. Acad. Sci. USA *90*, 4261–4265.

Chu, Y.W., Seftor, E.A., Romer, L.H., and Hendrix, M.J. (1996). Experimental coexpression of vimentin and keratin intermediate filaments in human melanoma cells augments motility. Am. J. Pathol. *148*, 63–69.

Clark, R.A.F. (1993). Mechanisms of cutaneous wound repair. In: Dermatology in General Medicine, Vol. I, ed. T.B. Fitzpatrick, A.Z. Eisen, K. Wolff, I.M. Freedberg, and M.D. Austen, New York, NY: McGraw-Hill Book Company, 473–486.

Cohen, I.K., and Mast, B.A. (1990). Models of wound healing. J. Trauma *30*, S149–155.

Coulombe, P.A. (1993). The cellular and molecular biology of keratins: beginning a new era. Curr. Opin. Cell Biol. *5*, 17–29.

Coulombe, P.A. (1997). Towards a molecular definition of keratinocyte activation after acute injury to stratified epithelia. Biochem. Biophys. Res. Commun. *236*, 231–238.

Coulombe, P.A., Bravo, N.S., Paladini, R.D., Nguyen, D., and Takahashi, K. (1995). Overexpression of human keratin 16 produces a distinct phenotype in transgenic mouse skin. Biochem. Cell Biol. *73*, 611–618.

Eckes, B., et al. (1998). Impaired mechanical stability, migration and contractile capacity in vimentin-deficient fibroblasts. J. Cell Sci. *111*, 1897–1907.

Fang, K.S., Ionides, E., Oster, G., Nuccitelli, R., and Isseroff, R.R. (1999). Epidermal growth factor receptor relocalization and kinase activity are necessary for directional migration of keratinocytes in DC electric fields. J. Cell Sci. *112*, 1967–1978.

Fuchs, E., and Cleveland, D.W. (1998). A structural scaffolding of intermediate filaments in health and disease. Science *279*, 514–519.

Fuchs, E., and Weber, K. (1994). Intermediate filaments: structure, dynamics, function, and disease. Annu. Rev. Biochem. *63*, 345–382.

Galou, M., Colucci-Guyon, E., Ensergueix, D., Ridet, J.L., Gimenez y Ribotta, M., Privat, A., Babinet, C., and Dupouey, P. (1996). Disrupted glial fibrillary acidic protein network in astrocytes from vimentin knockout mice. J. Cell Biol. *133*, 853–863.

Garlick, J.A., and Taichman, L.B. (1994). Fate of human keratinocytes during reepithelialization in an organotypic culture model. Lab. Invest. *70*, 916–924.

Grinnell, F. (1992). Wound repair, keratinocyte activation and integrin modulation. J. Cell Sci. *101*, 1–5.

Hogan, B., Beddington, R., Costantini, F., and Lacy, E. (1994). Manipulating the mouse embryo: A laboratory manual, Plainview, NY: Cold Spring Harbor Press, 497.

Hutton, E., Paladini, R.D., Yu, Q.C., Yen, M.-Y., Coulombe, P.A., and Fuchs, E. (1998). Functional differences between keratins of stratified and simple epithelia. J. Cell Biol. *143*, 1–13.

Jacinto, A., Martinez-Arias, A., and Martin, P. (2001). Mechanisms of epithelial fusion and repair Nat. Cell Biol. *3*, E117–E123.

Julien, J.P. (1999). Neurofilament functions in health and disease. Curr. Opin Neurobiol. *9*, 554–560.

Krawczyk, W.S. (1971). A pattern of epidermal cell migration during wound healing. J. Cell Biol. *49*, 247–263.

Ku, N.O., Might, S., Toshima, R.G., and Ovary, MB (1995). Chronic hepatitis, hepatocyte fragility, and increased soluble phosphoglycokeratins in transgenic mice expressing a keratin 18 conserved arginine mutant. J. Cell Biol. *131*, 1303–1314.

Ku, N.O., Michie, S.A., Soetikno, R.M., Resurreccion, E.Z., Broome, R.L., and Omary, M.B. (1998). Mutation of a major keratin phosphorylation site predisposes to hepatotoxic injury in transgenic mice. J. Cell Biol. *143*, 2023–2032.

Ku, N.O., Michie, S.A., Soetikno, R.M., Resurreccion, E.Z., Broome, R.L., Oshima, R.G., and Omary, M.B. (1996). Susceptibility to hepatotoxicity in transgenic mice that express a dominant-negative human keratin 18 mutant. J. Clin. Invest. *98*, 1034–1046.

Ku, N.O., Wright, T.L., Terrault, N.A., Gish, R., and Omary, M.B. (1997). Mutation of human keratin 18 in association with cryptogenic cirrhosis. J. Clin. Invest. *99*, 19–23.

Lampe, P.D., Nguyen, B.P., Gil, S., Usui, M., Olerud, J., Takada, Y., and Carter, W.G. (1998). Cellular interactions of interactions of integrin alpha3-beta1 with laminin-5 promotes gap junctional communication. J. Cell Biol. *143*, 1735–1747.

Ma, L., Yamada, S., Wirtz, D., and Coulombe, P.A. (2001). A 'hot-spot' mutation alters the mechanical properties of keratin filament networks. Nat. Cell Biol. *3*, 503–506.

Machesney, M., Tidman, N., Waseem, A., Kirby, L., and Leigh, I. (1998). Activated keratinocytes in the epidermis of hypertrophic scars. Am. J. Pathol. *152*, 1133–1141.

Magin, T.M., Schroder, R., Leitgeb, S., Wanninger, F., Zatloukal, K., Grund, C., and Melton, D.W. (1998). Lessons from keratin 18 knockout mice: formation of novel keratin filaments, secondary loss of keratin 7 and accumulation of liver-specific keratin 8-positive aggregates. J. Cell Biol. *140*, 1441–1451.

Mansbridge, J.N., and Knapp, A.M. (1987). Changes in keratinocyte maturation during wound healing. J. Invest. Dermatol. *89*, 253–263.

Martin, P. (1997). Wound healing—Aiming for the perfect skin regeneration. Science *276*, 75–81.

McGowan, K.M., and Coulombe, P.A. (1998a). Onset of keratin 17 expression coincides with the definition of major epithelial lineages during mouse skin development. J. Cell Biol. *143*, 469–486.

McGowan, K.M., and Coulombe, P.A. (1998b). The wound repair associated keratins 6, 16, and 17: insights into the role of intermediate filaments in specifying cytoarchitecture. In: Subcellular Biochemistry: Intermediate Filaments, ed. J.R. Harris and H. Herrmann, London: Plenum Publishing Co., 141–165.

Mellin, T.N., Cashen, D.E., Ronan, J.J., Murphy, B.S., DiSalvo, J., and Thomas, K.A. (1995). Acidic fibroblast growth factor accelerates dermal wound healing in diabetic mice. J. Invest. Dermatol. *104*, 850–855.

Missero, C., Di Cunto, F., Kiyokawa, H., Koff, A., and Dotto, G.P. (1996). The absence of p21Cip1/WAF1 alters keratinocyte growth and differentiation and promotes ras-tumor progression. Genes Dev. *10*, 3065–3075.

Paladini, R.D., and Coulombe, P.A. (1998). Directed expression of keratin 16 to the progenitor basal cells of transgenic mouse skin delays skin maturation. J. Cell Biol. *142*, 1035–1051.

Paladini, R.D., and Coulombe, P.A. (1999). The functional diversity of epidermal keratins revealed by the partial rescue of the keratin 14 null phenotype by keratin 16. J. Cell Biol. *146*, 1185–1201.

Paladini, R.D., Takahashi, K., Bravo, N.S., and Coulombe, P.A. (1996). Onset of re-epithelialization after skin injury correlates with a reorganization of keratin filaments in wound edge keratinocytes: defining a potential role for keratin 16. J. Cell Biol. *132*, 381–397.

Pekny, M., Johansson, C.B., Eliasson, C., Stakeberg, J., Wallen, A., Perlmann, T., Lendahl, U., Betsholtz, C., Berthold, C.H., and Frisen, J. (1999). Abnormal reaction to central nervous system injury in mice lacking glial fibrillary acidic protein and vimentin. J. Cell Biol. *145*, 503–514.

Pilcher, B.K., Dumin, J., Schwartz, M.J., Mast, B.A., Schultz, G.S., Parks, W.C., and Welgus, H.G. (1999). Keratinocyte collagenase-1 expression requires an epidermal growth factor receptor autocrine mechanism. J. Biol. Chem. *274*, 10372–10381.

Porter, R.M., Hutcheson, A.M., Rugg, E.L., Quinlan, R.A., and Lane, E.B. (1998). cDNA cloning, expression, and assembly characteristics of mouse keratin 16. J. Biol. Chem. *273*, 32265–32272.

Purkis, P.E., Steel, J.B., Mackenzie, I.C., Nathrath, W.B., Leigh, I.M., and Lane, E.B. (1990). Antibody markers of basal cells in complex epithelia. J. Cell Sci. *97*, 39–50.

Rouabhia, M., Germain, L., Belanger, F., and Auger, F.A. (1993). Cultured epithelium allografts: Langerhans cell and Thy-1^+ dendritic epidermal cell depletion effects on allograft rejection. Transplantation *56*, 259–264.

Stoscheck, C.M., Nanney, L.B., and King, L.E., Jr. (1992). Quantitative determination of EGF-R during epidermal wound healing. J. Invest. Dermatol. *99*, 645–649.

Takahashi, K., and Coulombe, P.A. (1996). A transgenic mouse model with an inducible skin blistering disease phenotype. Proc. Natl. Acad. Sci. USA *93*, 14776–14781.

Takahashi, K., and Coulombe, P.A. (1997). Defining a region of the human keratin 6a gene that confers inducible expression in stratified epithelia of transgenic mice. J. Biol. Chem. *272*, 11979–11985.

Takahashi, K., Coulombe, P.A., and Miyachi, Y. (1999). Using transgenic models to study the pathogenesis of keratin-based inherited diseases. J. Dermatol. Sci. *21*, 73–95.

Takahashi, K., Folmer, J., and Coulombe, P.A. (1994). Increased expression of keratin 16 causes anomalies in cytoarchitecture and keratinization in transgenic mouse skin. J. Cell Biol. *127*, 505–520.

Takahashi, K., Yan, B., Yamanishi, K., Imamura, S., and Coulombe, P.A. (1998). The two functional type II keratin 6 genes of mouse show a differential regulation and evolved independently from their human orthologs. Genomics *53*, 170–183.

Wawersik, M., and Coulombe, P.A. (2000). Forced expression of keratin 16 alters the adhesion, differentiation, and migration of mouse skin keratinocytes. Mol. Biol. Cell *11*, 3315–3327.

Wawersik, M., Paladini, R.D., Noensie, E., and Coulombe, P.A. (1997). A proline residue in the a-helical rod domain of type I keratin 16 destabilizes keratin heterotetramers and influences incorporation into filaments. J. Biol. Chem. *272*, 32557–32565.

Wojcik, S.M., Bundman, D.S., and Roop, D.R. (2000). Delayed wound healing in keratin 6a knockout mice. Mol. Cell. Biol. *20*, 5248–5255.

Zatloukal, K., Stumptner, C., Lehner, M., Denk, H., Baribault, H., Eshkind, L.G., and Franke, W.W. (2000). Cytokeratin 8 protects from hepatotoxicity, and its ratio to cytokeratin 18 determines the ability of hepatocytes to form Mallory bodies. Am. J. Pathol. *156*, 1263–1274.